Fundamental Properties of Mie Resonances in Water Spheres

Jacobsen, Rasmus Elkjær; Arslanagic, Samel; Laurynenka, Andrei

Published in:
Proceedings of 2019 International Symposium on Electromagnetic Theory

Link to article, DOI:
10.23919/ursi-emts.2019.8931459

Publication date:
2019

Document Version
Peer reviewed version

URSI EM Theory Symposium, EMTS 2019, San Diego, CA, 27– 31 May 2019

Fundamental Properties of Mie Resonances in Water Spheres

Rasmus E. Jacobsen* (1), Samel Arslanagić (2), and Andrei V. Lavrinenko (3)
(1), (3) Department of Photonics Engineering, Technical University of Denmark, Kongens Lyngby, 2800, Denmark,
e-mail: (1) rajac@fotonik.dtu.dk, (3) alav@fotonik.dtu.dk,
(2) Department of Electrical Engineering, Technical University of Denmark, Kongens Lyngby, 2800, Denmark,
e-mail: sar@elektro.dtu.dk

Abstract

All-dielectric metamaterials constitute an interesting route in the artificial material design due to their low-loss properties. Such constructs require high permittivity materials which support the excitation of Mie resonances, thereby enabling the underlying inclusions to be of small electrical sizes. Optics mostly relies on silicon, while several materials are used in the microwave range. Presently, we consider the potential of simple water as the inclusion in practical artificial materials due to its high permittivity and tunable dynamic properties through e.g., frequency and temperature variations. To this end, we undertake an analytical study of Mie resonances in water spheres and examine primarily the effects of frequency and temperature variation on the excitation and isolation of electric and magnetic dipoles. We also demonstrate directive patterns in forward and backward directions in water spheres with balanced electric/magnetic dipole excitations. As such, our results may not only be used directly in or as a guideline for metamaterial design, but they may also pave the way for simple and directive antennas.

1. Introduction

All-dielectric metamaterials (MMs) are a growing trend in photonics and electromagnetics in which high permittivity inclusions are employed in low index matrices to excite Mie resonances [1]. It has recently been shown that water can be used as an alternative material for inclusions of all-dielectric MMs and metasurfaces (MSs) due to its advantageous properties as bio-friendliness, abundancy, inexpensiveness and high permittivity in the microwave range [2-5]. Water-based MMs can be tuned thermally by heating/cooling of elements due to its temperature-dependent permittivity [2, 6-7], and mechanically by reshaping/deforming its volume or rotating partially filled containers [2, 8]. Even chemical reactions can be applied for designing of reconfigurable systems [9]. On the other hand, a great variety of water-based MSs with rather broadband and high absorbance have been reported recently [10-11]. Placing a metallic layer behind the surface effectively removes the transmittance, thereby enhancing the absorbance. Another type of MS consisting of 'rod-like' water-elements in a foam material was shown to have reflection and transmission modulation capabilities through a simple mechanical rotation of the surface [5]. The modulation was improved significantly by stacking several MSs in a multilayer array.

Thus far, most of the studies on water-based structures were performed for 2-D and 3-D arrays using numerical tools. Presently, we examine the properties of electric and magnetic dipole resonances (Mie resonances) in isolated water spheres. The spherical geometry constitutes a well-known canonical problem which can be treated analytically using spherical vector wave formulation. With the analytical solution at hand, a range of fundamental properties and effects of water spheres may easily be revealed. Particular attention is devoted to the potential of such water spheres to support both isolated (for MM design) as well as balanced (for directive antenna design) dipole resonances, and to assess their behaviors with frequency and temperature change of the water permittivity. Throughout the paper, we consider a plane wave illumination of a water sphere at low frequencies mainly where the losses in water are low enough so that strong and isolated resonances can be excited. We show that the resonances at room temperature results in low scattering and high absorption due to the losses in water. Increasing the temperature effectively reduces the losses and therefore improves the intensity and isolation of the resonances. At last, we show that Kerker's conditions can be satisfied at non-resonant frequencies resulting in mainly forward or backward scattering. Throughout the work, the time-factor exp $(j\omega t)$, with ω being the angular frequency and t being the time, is assumed and suppressed.

2. Configuration and analytical expressions

The water sphere of radius r_s is situated in free-space and is illuminated by a linearly polarized plane wave with the electric (magnetic) field $\mathbf{E}^i$ ($\mathbf{H}^i$) as shown in Figure 1(a). A Cartesian coordinate system (x, y, z), with its associated spherical coordinate system (r, θ, ϕ), is placed with the origin placed at the center of the sphere. The solution to the spherical wave expansion of internal ($\mathbf{E}^w$, $\mathbf{H}^w$) and scattered ($\mathbf{E}^s$, $\mathbf{H}^s$) fields is well-known, and the amplitude coefficients of the fields are [12, Sec. 4.3]

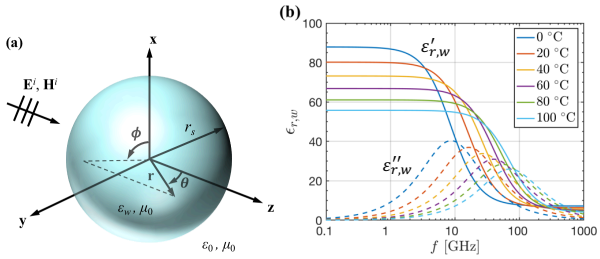

Figure 1. (a) Sketch of the water sphere in free-space illuminated by a plane wave and **(b)** relative permittvity of water as a function of frequency and temperature.

$$a_n = \frac{\varepsilon_{r,w} j_n(k_w r_s) j_n{}'(k_0 r_s) - j_n{}'(k_w r_s) j_n(k_0 r_s)}{\varepsilon_{r,w} j_n(k_w r_s) h_n^{(2)\prime}(k_0 r_s) - j_n{}'(k_w r_s) h_n^{(2)}(k_0 r_s)} \quad (1)$$

$$b_n = \frac{j_n(k_w r_s) j_n{}'(k_0 r_s) - j_n{}'(k_w r_s) j_n(k_0 r_s)}{j_n(k_w r_s) h_n^{(2)\prime}(k_0 r_s) - j_n{}'(k_w r_s) h_n^{(2)}(k_0 r_s)} \quad (2)$$

$$c_n = \frac{\varepsilon_{r,w}^{1/2}\left[j_n(k_0 r_s) h_n^{(2)\prime}(k_0 r_s) - j_n{}'(k_0 r_s) h_n^{(2)}(k_0 r_s)\right]}{\varepsilon_{r,w} j_n(k_w r_s) h_n^{(2)\prime}(k_0 r_s) - j_n{}'(k_w r_s) h_n^{(2)}(k_0 r_s)} \quad (3)$$

$$d_n = \frac{j_n(k_0 r_s) h_n^{(2)\prime}(k_0 r_s) - j_n{}'(k_0 r_s) h_n^{(2)}(k_0 r_s)}{j_n(k_w r_s) h_n^{(2)\prime}(k_0 r_s) - j_n{}'(k_w r_s) h_n^{(2)}(k_0 r_s)} \quad (4)$$

where a_n and b_n (c_n and d_n) are the coefficients of the TM^r and TE^r field components, respectively, of the scattered (internal) fields. k_w and k_0 are the wavenumbers in water and free-space, respectively, while j_n and $h_n^{(2)}$ are the nth order spherical Bessel function of the first kind and spherical Hankel function of the second kind, respectively. The prime $'$ denotes the operation $g_n{}'(x) = d[x g_n(x)]/dx$.

The absorption, extinction and scattering efficiencies are used to describe the response of the sphere, and they are related by [12, Sec. 3.4]

$$Q_{\mathrm{abs}} = Q_{\mathrm{ext}} - Q_{\mathrm{sca}} \quad (5)$$

where

$$Q_{\mathrm{sca}} = \frac{2}{(k_0 r_s)^2} \sum_{n=1}^{\infty} (2n+1)(|a_n|^2 + |b_n|^2) \quad (6)$$

$$Q_{\mathrm{ext}} = \frac{2}{(k_0 r_s)^2} \sum_{n=1}^{\infty} (2n+1)\mathrm{Re}\{a_n + b_n\} \quad (7)$$

The induced electric ($\mathbf{p}$ [C·m]) and magnetic ($\mathbf{m}$ [A·m^2]) dipole moments ($n = 1$) can be determined by the volume integrals [13]

$$\mathbf{p} = \frac{1}{j\omega} \int_V \mathbf{J}_d \, dv', \quad \mathbf{m} = \frac{1}{2} \int_V \mathbf{r}' \times \mathbf{J}_d \, dv' \quad (8)$$

with $\mathbf{J}_d = j\omega\varepsilon_0(\varepsilon_{r,w} - 1)\mathbf{E}^w$ being the polarization current density inside the water sphere, V being the volume of the sphere, dv' being the differential volume element and $\mathbf{r}'$ denoting the position vector. Performing the integrations, one obtains the following

$$\mathbf{p} = \hat{\mathbf{e}}_E 4\pi r_s^3 \varepsilon_0 (\varepsilon_{r,w} - 1) E_0 c_1 \frac{j_1(k_w r_s)}{k_w r_s} \quad (9)$$

$$\mathbf{m} = \hat{\mathbf{k}}_E \times \hat{\mathbf{e}}_E 2\pi r_s^4 \omega \varepsilon_0 (\varepsilon_{r,w} - 1) E_0 d_1 \frac{j_2(k_w r_s)}{k_w r_s} \quad (10)$$

where $\hat{\mathbf{e}}_E$ and $\hat{\mathbf{k}}_E$ are the unit vectors of the incident electric field and wave vector, respectively.

In the temperature range from 0 to 100 °C and under normal pressure, water is a liquid; it thus adopts the body of a provided container as well as preserves its volume. The highly temperature dependent dielectric permittivity is described by the Debye formula [2, 6]

$$\varepsilon_{r,w}(\omega, T) = \varepsilon'_{r,w} - j\varepsilon''_{r,w} = \varepsilon_\infty(T) + \frac{\varepsilon_s(T) - \varepsilon_\infty(T)}{1 - j\omega\tau(T)} \quad (11)$$

with T [°C] being the temperature of water. $\varepsilon_\infty(T)$ and $\varepsilon_s(T)$ are the optical and static permittivities, respectively, while $\tau(T)$ is the rotational relaxation time. The relative permittivity of pure water is shown in Figure 1(b).

3. Resonant water sphere

In this section, we consider a sphere with a radius of 21.6 mm and an x-polarized incident plane wave of amplitude E_0 [V/m] travelling in the positive z-direction. At first, the temperature is kept at $T = 20$ °C and the resulting absorption and scattering efficiencies as functions of frequency are shown in Figure 2(a). The scattering efficiency calculated in COMSOL is included for validation.

The first two peaks of the absorption efficiency are due to the induced magnetic (0.767 GHz) and electric (1.092 GHz) dipole resonance. This is confirmed by magnetic and electric dipole moments shown in Figure 2(b) as well as the field profiles shown in Figure 2(c) and (d). The curve of the scattering efficiency has a pronounced peak coming from the magnetic dipole resonance, while the electric dipole only gives rise to a small increase in the scattering efficiency. Both of the resonances do not make the scattering efficiency exceed that found in the optical region. However, the absorption efficiency is significantly increased by the resonances making it exceed that found at non-resonant frequencies i.e. frequencies below 0.7 GHz and above 5 GHz. Since the absorbed power in water is related to the ohmic heating by $P_{\mathrm{abs}} = 0.5\omega\varepsilon_0\varepsilon''_{r,w} \int_V |\mathbf{E}^w|^2 \, dv'$, the internal fields, and hence the induced dipoles, must be strong.

In the homogenization of artificial materials, usually it is important to have well-isolated (non-coupling) dipole resonances. The isolation of the induced dipoles is shown in Figure 3(a) by the magnitude of the internal coefficients for their first and second modes. The magnetic dipole (d_1) at the resonance is well-isolated, while the electric dipole

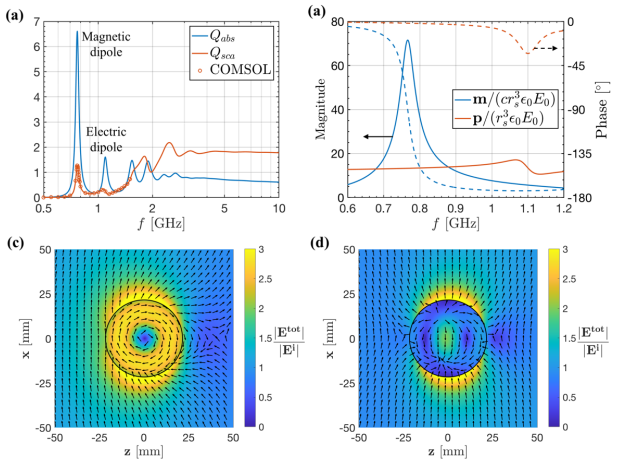

Figure 2. Sphere with $r_s = 21.6$ mm: **(a)** the absorption and the scattering efficiencies as functions of frequency (logarithmic scale); **(b)** the magnitude and phase of the normalized induced magnetic and electric dipole moments as functions of frequency; **(c)** and **(d)** the magnitude of the total electric field normalized with that of the incident at the frequencies 0.767 and 1.092 GHz, respectively, in the *xz*-plane. The arrows indicate the direction of the electric field.

(c_1) is not, due to the presence of the magnetic dipole and quadrupole.

In Figure 4, the effects of the temperature and frequency variation on the scattering and absorption efficiencies, as well as the magnetic and electric dipole moments, are examined. Clearly, the resonances are more pronounced at higher temperatures causing higher efficiencies as well as better isolated resonances (see Figure 3(b)). Especially at the magnetic dipole resonance the scattering efficiency increases from 0.4 to 9.7 with a temperature increase from 0 to 100 °C, while the absorption efficiency increases from 4.2 to 9.5 from 0 to 70 °C. This behavior is due to the decrease of $\varepsilon''_{r,w}$: at 0.767 (1.092) GHz and $T = 20$ °C, $\varepsilon''_{r,w} \approx 3.4$ (4.9), while at $T = 40$ °C, it has dropped to 1.9 (2.7). From this, we could state that the absorption efficiency should decrease by an increase in temperature. However, we observe the opposite behavior due to the enhancement of the dipole moments (i.e. internal fields) as seen in Figure 4(c) and (d). Besides the more pronounced induced resonances, increasing the temperature causes a blue-shift of the spectrum due to the decrease of $\varepsilon'_{r,w}$. This blue-shift corresponds to approximately 190 MHz (25 %)

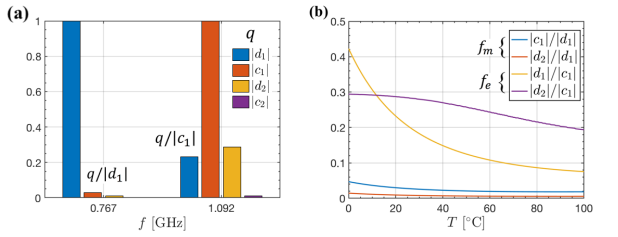

Figure 3. Isolation of resonances shown by internal coefficients at the magnetic (f_m) and electric (f_e) dipole resonance frequencies in **(a)** for 0 °C and **(b)** 0–100 °C.

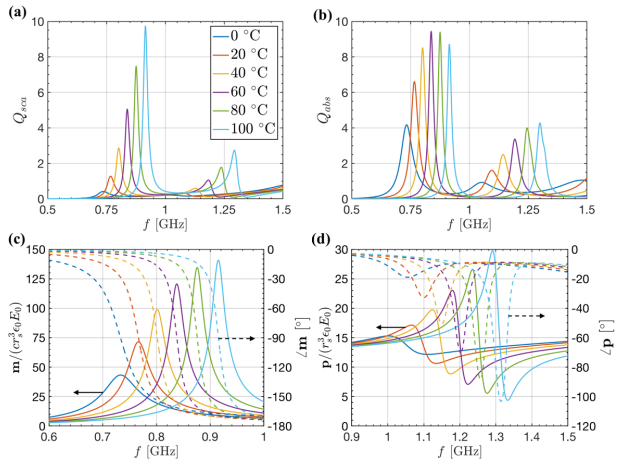

Figure 4. Variation of temperature. Sphere with $r_s = 21.6$ mm showing the **(a)** scattering efficiency, **(b)** absorption efficiency, **(c)** magnetic dipole moment and **(d)** electric dipole moment as functions of frequency and temperature.

of the magnetic dipole resonance frequency with an increase in the temperature from 0 to 100 °C.

In general, the maximum absorption ($Q_{\text{abs}} \approx 13.6$) in a water sphere is found for $r_s \approx 288$ mm at $T = 0$ °C, and is due to a magnetic dipole resonance at 80 MHz. The maximum scattering efficiency is found for $f \to 0$ Hz since $\varepsilon''_{r,w} \to 0$. Smaller spheres exhibiting dipole resonances at higher frequencies have much less profound resonances and efficiencies compared that investigated in Figure 2-5. E.g. a water sphere with $r_s \approx 3.3$ mm at 20 °C exhibits a magnetic dipole resonance at 5 GHz, but has a scattering (absorption) efficiency less than 0.1 (1.5). Increasing the temperature brings a dramatic enhancement to the induced resonances due to the decrease of $\varepsilon''_{r,w}$.

The losses in water must be low enough to achieve pronounced and well-isolated resonances if water-inclusions are to be used in MMs and MSs. Generally, this is achieved at low frequencies and/or high temperatures.

Several ways to maximize the scattering in one direction have been proposed, where recently a directive antenna with a needle-like radiation pattern has been demonstrated theoretically in [14]. In our simple configuration, it is possible to attain directed scattering as well by satisfying Kerker's conditions. The dipole moments (magnitude and phase) shown in Figure 2(b) and 3(c)-(d) are normalized as $\mathbf{m}/(c{r_s}^3\varepsilon_0E_0)$ and $\mathbf{p}/({r_s}^3\varepsilon_0E_0)$, where c is the speed of light, since the difference in their units is [m/s]. When $m/p = c$ (where $\mathbf{p} = \hat{\mathbf{e}}_E p$ and $\mathbf{m} = \hat{\mathbf{k}}_E \times \hat{\mathbf{e}}_E m$), then the scattering will be maximized in the forward direction, while if $m/p = -c$, it will be in the backward direction. These cases are marked by the black circles in Figure 2(a). In Figure 5, the normalized differential scattering cross section [12, Sec. 3.4] is shown at these frequencies as well as the magnetic dipole resonance frequency. Such effects are interesting in MMs, MSs and directive antennas designs, since only forward (backward) scattering

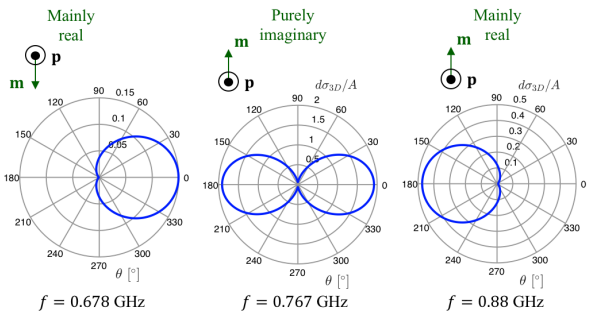

Figure 5. Normalized differential scattering cross section at 0.678, 0.767 and 0.88 GHz.

corresponds to zero reflection (transmission). The frequency of the forward scattering can be controlled by the temperature and size of the sphere. For enhanced forward scattering, a different shape could be pursued, where the magnetic and electric dipoles (or higher order multipole moments [15]) are overlapping. Here, it is important that the dipoles have the right orientation and the losses in water are minimal, so that not all the energy is absorbed [10-11].

4. Conclusions

We investigated the performance of a water sphere resonant around 1 GHz. The spectrum of the absorption and scattering efficiencies as well as the induced magnetic and electric dipole moments were calculated using analytical expressions provided in Section 2. The magnetic dipole resonance was the most profound and isolated resulting in enhanced scattering and absorption. However, due to the losses in water at room temperature, most of the energy was absorbed by it. An increase in temperature resulted in both more profound and isolated resonances, all desirable features for a prospective MM and MS design. The temperature increases also lead to higher efficiencies (especially in scattering), and blue-shifted the spectrum due to the decrease in the dielectric constant of water. Smaller spheres resonating at higher frequencies, where losses are even higher, were also briefly discussed. Moreover, we demonstrated designs with balanced magnetic and electric dipole moments which resulted in primarily forward or backward scattering. The observed effects are very interesting not only in the area of artificial material design, but also for the design of directive electrically small antennas utilizing such simple materials as pure water.

5. References

1. S. Jahani, and Z. Jacob, “All-dielectric meta-materials,” Nat. Nanotechnol., **11**, pp 23–36, 2016.

2. A. Andryieuski, S. M. Kuznetsova, S. V. Zhukovsky, Y. S. Kivshar, and A. V. Lavrinenko, “Water: promising opportunities for tunable alldielectric electromagnetic metamaterials,” Sci. Rep., **5**, 13535, 2015.

3. Y. J. Yoo, S. Ju, S. Y. Park, Y. J. Kim, J. Bong, T. Lim, K. W. Kim, J. Y. Rhee, and Y. P. Lee, “Metamaterial absorber for electromagnetic waves in periodic water droplets,” Sci. Rep., **5**, 14018, 2015.

4. X. Cai, S. Zhao, M. Hu, J. Xiao, N. Zhang, and J. Yang, “Water based fluidic radio frequency metamaterials”, J. Appl. Phys., **122**, 184101, 2017.

5. R. E. Jacobsen, A. V. Lavrinenko and S. Arslanagić, "Water-Based Metasurfaces for Effective Switching of Microwaves," IEEE Antennas Wirel. Propag. Lett., **17**, 4, 2018, pp. 571-574.

6. W. Ellison, “Permittivity of pure water, at standard atmospheric pressure, over the frequency range 0-25 thz and the temperature range 0-100 c,” J. Phys. Chem. Ref. Data, **36**, 2007, pp 1–18.

7. M. V. Rybin, D. S. Filonov, P. A. Belov, Y. S. Kivshar, and M. F. Limonov, “Switching from Visibility to Invisibility via Fano Resonances: Theory and Experiment,” Sci. Rep., **5**, 8774, 2015.

8. M. Odit, P. Kapitanova, A. Andryieuski, P. Belov, and A. V. Lavrinenko, ”Experimental demonstration of water based tunable metasurface,” Appl. Phys. Lett., **109**, 011901, 2016.

9. X. Yang, D. Zhang, S. Wu, Y. Yin, L. Li, K. Cao, and K. Huang, “Reconfigurable all-dielectric metasurface based on tunable chemical systems in aqueous solution,” Sci. Rep., **7**, 3190, 2017.

10. J. Ren, and J. Y. Yin. “Cylindrical-Water-Resonator-Based Ultra-Broadband Microwave Absorber,” Optical Materials Express **8**, 8, 2018, pp. 2060–2071.

11. Q. Song et al., ”Water- Resonator-Based Metasurface: An Ultrabroadband and Near-Unity Absorption,” Adv. Opt. Mater., **5**, 1601103, 2017.

12. C. F. Bohren, and D. R. Huffman, “Absorption and Scattering of Light by Small Particles,” Wiley, 1983.

13. A. Dirksen, S. Arslanagic, and O. Breinbjerg, ”Resonances and dipole moments in dielectric, magnetic and magnetodielectric cylinders – an overview,” Appl. Phys. A, **103**, 2011.

14. R. W. Ziolkowski, ”Using Huygens Multipole Arrays to Realize Unidirectional Needle-Like Radiation,” Phys. Rev. X, **7**, 3, 031017, 2017.

15. R. Alaee, R. Filter, D. Lehr, F. Lederer, C. Rockstuhl, ”A generalized Kerker condition for highly directive nanoantennas,” Opt. Lett, **40**, 11, 2015, pp. 2645-2648.